

Host Properties of Cucurbit[7]uril: Fluorescence Enhancement of Anilinonaphthalene Sulfonates

Brian D. Wagner,^{*,†} Natasa Stojanovic,[†] Anthony I. Day,[‡] and Rodney J. Blanch^{*,‡}

Department of Chemistry, University of Prince Edward Island, Charlottetown, P.E.I., Canada C1A 4P3, and School of Chemistry, University College, University of New South Wales, Australian Defense Force Academy, Canberra ACT, Australia

Received: April 4, 2003; In Final Form: July 3, 2003

This work describes the fluorescence enhancement of the probes 2,6- and 1,8-ANS via complexation with the macrocyclic host cucurbit[7]uril (Q7). The association of these two guests with the Q7 host has been studied using fluorescence, ¹H NMR spectroscopy, and molecular modeling. In the case of 2,6-ANS, 1:1 inclusion complexes are formed via inclusion of the phenyl moiety into the Q7 cavity (as confirmed by NMR), with a large fluorescence enhancement of a factor of 25 ± 3 and an association constant of $600 \pm 150 \text{ M}^{-1}$. These values are significantly larger than those reported in the literature for 2,6-ANS inclusion into cucurbit[6]uril (Q6); for example, the association constant is larger by over an order of magnitude, indicating the superior host abilities of Q7 as compared to its smaller homologue. These results are significant, as they provide the first direct comparison of the host abilities of Q6 and Q7. In the case of 1,8-ANS, very large fluorescence enhancement was also observed upon addition of Q7. The enhancement as a function of Q7 concentration indicated the formation of a 2:1 host:guest complex. However, host–guest inclusion was not observed via NMR. Thus, a 2:1 complex where 1,8-ANS is sandwiched between the outer surface of two Q7 molecules is proposed. Such complexation is supported by semiempirical PM3 calculations, and the resulting minimized structures are reminiscent of the structure of the solid exclusion compound of 1,8-ANS and Q6 previously reported in the literature.

Introduction

Cucurbituril^{1–4} is an interesting cage compound consisting of a σ -bonded C,N framework, with two opposing portals defined by carbonyl groups. It is a very rigid cage, consisting of six glycoluril monomers joined by pairs of methylene bridges. The presence of the internal cavity, accessible by these two openings, makes this molecule interesting, as it can serve as a host for the inclusion of smaller guest molecules. The host–guest inclusion complexes of cucurbituril in solution have been extensively studied in recent years, using NMR,^{5–12} X-ray crystallography,^{9,13,14} calorimetry,^{15–18} and UV–vis^{6,19–21} and fluorescence²² spectroscopy. A wide range of guests have been shown to become included within cucurbituril, including cations (e.g., alkyl- and aryl-substituted ammonium ions,^{5–7,15,19} metal ions,^{14,16,19} and protonated amines^{8,12,17}), neutral species (e.g., THF,^{9,10} Xe,^{10,11} trifluoroacetic acid,¹⁰ organic dyes,²⁰ and surfactants¹⁸), and anions (2,6-anilinonaphthalene sulfonate²²); this indicates the versatility and potential usefulness of cucurbituril as a host molecule.

Recently, the synthesis of a series of cucurbituril homologues has been reported,²³ with varying numbers of glycoluril monomers in the macrocycle. These are referred to as cucurbit-[*n*]uril²⁴ (Q_{*n*}), where *n* is the number of glycoluril monomers. Thus, cucurbituril itself is cucurbit[6]uril, or Q6. The *n* = 5, 7, 8, and 10 homologues have been successfully synthesized and characterized^{23,24} (the synthesis of decamethylated Q5 was

reported in 1992²⁵). These represent an exciting contribution to the area of host–guest chemistry, especially in the cases of Q7 and Q8, as these homologues have much larger internal cavities and portals and thus can be expected to have much improved host abilities as compared to cucurbituril itself. Q7 has an internal cavity with a diameter of 7.3 Å and a portal diameter of 5.4 Å, both being significantly larger than the Q6 cavity and portal diameters of 5.8 and 3.9 Å, respectively.²³

Buschmann and co-workers have published a number of papers on the inclusion complexes of Q5 and its decamethylated derivative (as well as Q6)^{26–29} and have reported association constants for the inclusion of alkali, alkaline earth, and ammonium ions,²⁷ transition metal ions,²⁶ and amines,²⁸ as well as complexes of Q5 and Q6 with cyclodextrins.²⁹ Kim and co-workers have reported on inclusion complexes of Q8, with hetero charge transfer pairs,³⁰ macrocycles,³¹ and (*E*)-diaminostilbene³² as guests. There have also been a few experimental studies of inclusion complexes of Q7, with the guests 2,6-bis-(4,5-dihydro-1*H*-imidazol-2-yl)naphthalene (in the original synthesis paper²³), SnCl₄(OH)₂,³³ 2,3-diazabicyclo[2.2.2]oct-2-ene (DBO),³⁴ *o*-carborane,³⁵ and viologens.^{36,37} Of these, the effect of Q7 on the fluorescence of a guest was reported only in the DBO study, and in that case only the effect on the fluorescence maximum of the guest was measured (allowing for the determination of the polarizability inside the Q7 cavity). Furthermore, out of these previous Q7 studies, binding constants have been reported only in the case of viologens. This is in marked contrast to the large number of association constants reported for inclusion into Q6, and the recent studies on Q5 and Q8, and is rather surprising considering that Q7 is the most soluble of the cucurbituril hosts and has a cavity size similar to that of

* To whom correspondence should be addressed. E-mail: bwagner@upeu.ca.

[†] University of Prince Edward Island.

[‡] University of New South Wales.

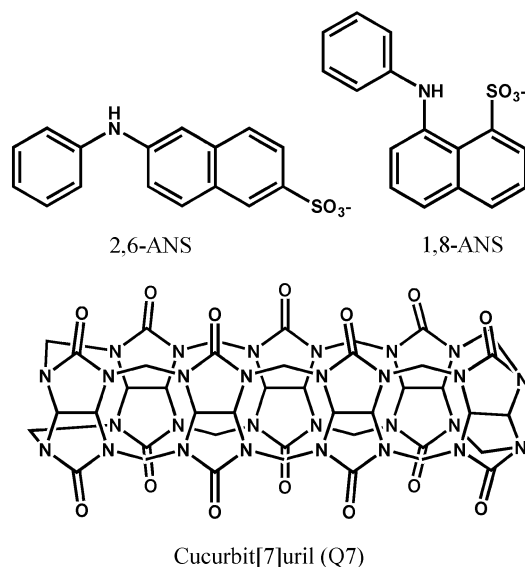


Figure 1. Molecular structures of the fluorescent guest molecules 2,6-ANS and 1,8-ANS and the host molecule cucurbit[7]uril.

β -cyclodextrin, making Q7 the most potentially useful of all the cucurbit[*n*]urils as a host. There has been a recent theoretical study³⁸ on the inclusion complex of Q7 with the same substituted naphthalene guest studied experimentally by Kim et al.²³ Their calculations supported the NMR results indicating that inclusion occurs with this host–guest pair and further indicated that in addition to van der Waals interaction and the hydrophobic effect hydrogen bonding between guest hydrogens and the host carbonyls is also an important driving force for inclusion in these cucurbiturils.

In this paper, we present the first fluorescence enhancement study of the inclusion of guests into Q7, using the related probes 1-anilino-8-naphthalene-sulfonic acid (1,8-ANS) and 2-anilino-6-naphthalene-sulfonic acid (2,6-ANS), shown in Figure 1, and report association constants for the complexation of these two guests with Q7. We also use NMR spectroscopy and molecular modeling to complement the fluorescent work. We have previously reported fluorescence studies of the interaction of these two probes with Q6.^{22,39} This is important, as it allows for the first time for a direct comparison of the host abilities of Q6 and Q7 to be made. This paper also demonstrates for the first time that Q7 can significantly enhance the fluorescence of a guest species; this is important for the potential application of Q7 in fluorescent molecular sensor technology.

Results

2,6-ANS. The fluorescence spectrum of 2,6-ANS was found to increase significantly in intensity upon addition of Q7 to the solution, as shown in Figure 2. This increase in fluorescence indicates the formation of a host–guest inclusion complex of 2,6-ANS within the Q7 cavity. There was very little shifting of the spectrum, however, with a fluorescence maximum of 459 ± 2 nm in the absence of Q7 and 452 ± 2 nm in the presence of 10 mM Q7. The increased fluorescence intensity is quantified as the fluorescence enhancement, F/F_0 : the ratio of the integrated fluorescence spectrum in the presence of a specific concentration of Q7 to that in its absence. The dependence of the fluorescence enhancement on Q7 concentration is shown in Figure 3. Assuming that only a 1:1 host:guest complex is being formed, the following equation can be derived for the dependence of F/F_0 on initial host concentration $[Q7]_0$:⁴⁰

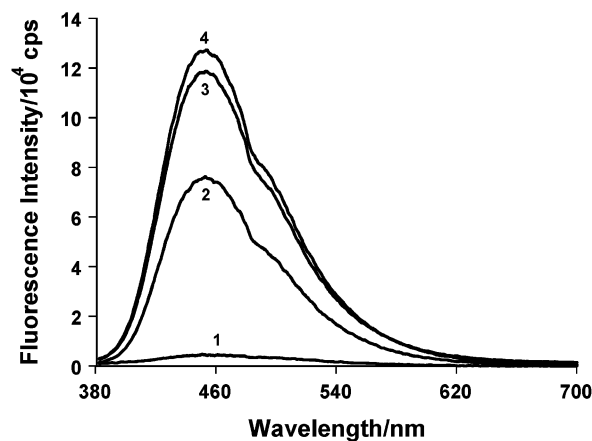


Figure 2. Fluorescence spectra of 2,6-ANS in the presence of various amounts of Q7: (1) 0 mM; (2) 2 mM; (3) 6 mM; (4) 10 mM.

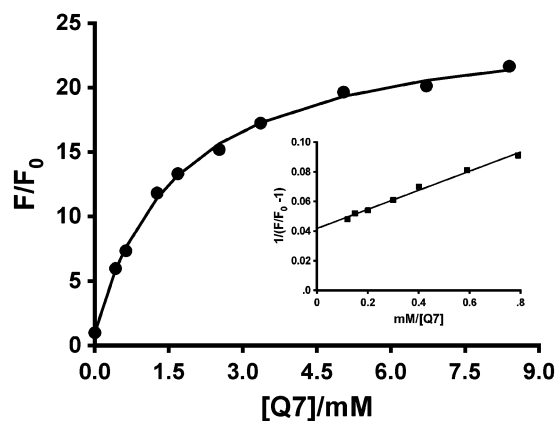


Figure 3. Fluorescence enhancement, F/F_0 , of 2,6-ANS as a function of Q7 concentration. The solid line shows the fit of the data to eq 1, with $K = 490 \text{ M}^{-1}$. The inset shows the linear double reciprocal plot indicating 1:1 complexation.

$$F/F_0 = 1 + (F_\infty/F_0 - 1) \frac{[Q7]_0 K}{(1 + [Q7]_0 K)} \quad (1)$$

where F_∞/F_0 is the fluorescence enhancement when all of the guest has been included and K is the equilibrium constant for 1:1 complexation ($H + G \rightleftharpoons H:G$). The measured data were found to fit very well to this equation, using a nonlinear least-squares procedure. This is shown in Figure 3, where the data points are the average values from three trials. The line of best fit, shown as the solid line in Figure 3, yielded a value of $K = 600 \pm 150 \text{ M}^{-1}$, with $F_\infty/F_0 = 25 \pm 3$. The assumption of 1:1 complexation was tested by plotting the double reciprocal plot of $1/(F/F_0 - 1)$ versus $1/[Q7]$; this plot will be nonlinear if higher-order inclusion complexes are formed. As shown in the inset of Figure 3, this plot was found to be linear ($R = 0.995$), confirming simple 1:1 host:guest complexation.

The interaction of 2,6-ANS with Q7 has also been studied with ¹H NMR. Figure 4 shows the ¹H NMR spectrum of 2,6-ANS as a function of Q7 concentration. In the presence of Q7, the 2,6-ANS resonances due to the phenyl moiety (peaks labeled g, h, i) initially broaden, while those signals attributed to the naphthalene moiety (peaks labeled a, b, d, e, f) are essentially unchanged. It should be noted that the resonance for the naphthalenic proton, c, also initially broadens. The phenyl signals continued to broaden and shift upfield with increasing Q7 concentration. Due to the extent of broadening, we are unable to accurately determine the magnitude of this upfield shift for the individual resonances. At these higher concentra-

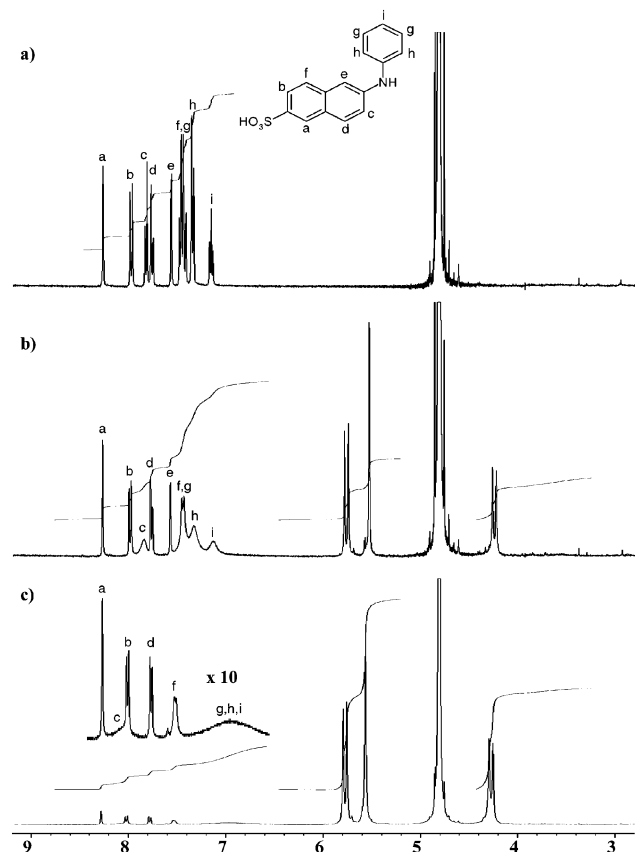


Figure 4. ^1H NMR spectrum of 2,6-ANS as a function of added Q7: (a) no Q7; (b) $\sim 1/6$ molar equiv of Q7; (c) ~ 1 molar equiv of Q7 (precipitation started to occur).

tions of Q7 the naphthalenic proton, c, has also broadened further, but it has moved ~ 0.3 ppm downfield, and the resonance due to proton e cannot be located. Unfortunately, we were unable to go to excess concentrations of Q7 due to coprecipitation of the compounds. The observed upfield shift is characteristic of molecules encapsulated in the cucurbit[*n*]uril cavity and indicates that the 2,6-ANS complexes with Q7 via encapsulation of the anilino group. The observed downfield shift of the naphthalenic proton, c, is characteristic of a proton sitting just outside the carbonyl portal.³

1,8-ANS. The fluorescence spectrum of 1,8-ANS was also found to increase significantly in intensity upon addition of Q7 to the solution, as shown in Figure 5, indicating the possible formation of a host–guest inclusion complex of 1,8-ANS within the Q7 cavity. Contrary to the case of 2,6-ANS, there was significant blue-shifting of the spectrum, with a fluorescence maximum of 517 ± 2 nm in the absence of Q7 and 469 ± 2 nm in the presence of 10 mM Q7. Figure 6 shows the plot of fluorescence enhancement as a function of Q7 concentration (averaged over three trials); this plot has a very different shape than that seen in Figure 3 for 2,6-ANS, suggesting the formation of higher-order complexes. This was confirmed by the double reciprocal plot shown in the inset of Figure 6, which is clearly nonlinear. The data in Figure 6 were thus fit to the following more complex equation for the formation of 1:1 and 2:1 host:guest complexes:⁴¹

$$F/F_0 = \frac{1 + F_1/F_0 K_1 [\text{Q7}]_0 + F_2/F_0 K_1 K_2 [\text{Q7}]_0^2}{(1 + K_1 [\text{Q7}]_0 + K_1 K_2 [\text{Q7}]_0^2)} \quad (2)$$

where F_1/F_0 and F_2/F_0 are the fluorescence intensities of the

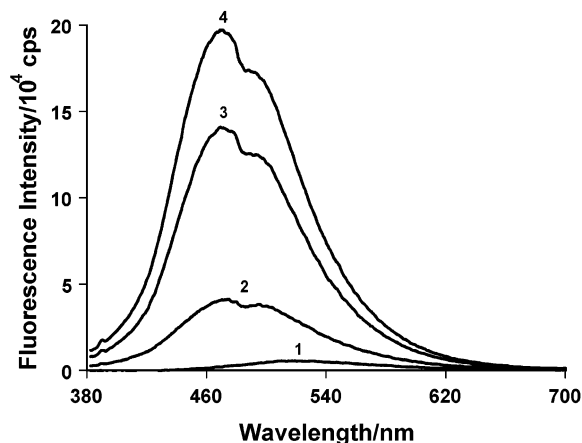


Figure 5. Fluorescence spectra of 1,8-ANS in the presence of various amounts of Q7: (1) 0 mM; (2) 2 mM; (3) 6 mM; (4) 10 mM.

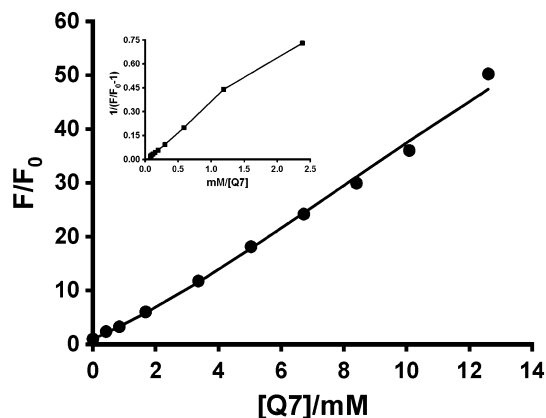


Figure 6. Fluorescence enhancement, F/F_0 , of 1,8-ANS as a function of Q7 concentration. The solid line shows the fit of the data to eq 2, with $K_1 = 14 \text{ M}^{-1}$ and $K_2 = 218 \text{ M}^{-1}$. The inset shows the nonlinear double reciprocal plot, indicating the formation of higher-order complexes.

1:1 and 2:1 complexes, respectively, relative to that of the free guest, K_1 is the equilibrium constant for formation of the 1:1 complex ($\text{H} + \text{G} \rightleftharpoons \text{H}:\text{G}$), and K_2 is the equilibrium constant for the formation of the 2:1 complex from addition of a second host to the 1:1 complex ($\text{H} + \text{H}:\text{G} \rightleftharpoons \text{H}_2:\text{G}$). The solid line in Figure 6 shows the excellent fit of the data to eq 2, yielding the values $F_1/F_0 = 110 \pm 75$, $F_2/F_0 = 94 \pm 34$, $K_1 = 19 \pm 4 \text{ M}^{-1}$, and $K_2 = 160 \pm 60 \text{ M}^{-1}$. By contrast, a much poorer fit was obtained using eq 1 for 1:1 complexation, as well as using the equation derived in the literature⁴² for 1:1 and 2:2 complexation.

The NMR studies of 1,8-ANS complexation were greatly hindered by the low solubility of the 1,8-ANS and by its coprecipitation with Q7 even at low concentrations. However, no signal broadening or chemical shift changes were observed during this titration, prior to loss of signal due to precipitation. This would indicate that there is little or no encapsulation of the 1,8-ANS by Q7 under these conditions.

Discussion

The fluorescence of 2,6-ANS is significantly enhanced by Q7, by a maximum factor of 25 at high Q7 concentration. The excellent fit of the enhancement as a function of Q7 concentration data to eq 1, and the linear double reciprocal plot indicate that simple 1:1 complexation is occurring between the 2,6-ANS guest and the Q7 host, with a moderately large association

constant of $600 \pm 150 \text{ M}^{-1}$. The lack of a significant blue-shift in the spectrum indicates that the mode of inclusion of 2,6-ANS into Q7 involves insertion of the phenyl moiety into the Q7 cavity, rather than the naphthalene moiety. This is confirmed by the NMR studies that show significant broadening and upfield shift of the phenyl protons, indicating both an intermediate rate of exchange and the insertion of the phenyl moiety into the cavity of the Q7. A much larger blue-shift of the 2,6-ANS spectrum would be expected if the naphthalene moiety was being included. For example, inclusion of 2,6-ANS into modified β -cyclodextrins, which involves naphthalene inclusion, results in a 28–40 nm blue-shift in the 2,6-ANS spectrum.⁴³ A similar mode of inclusion was also proposed for 2,6-ANS in Q6, which also formed 1:1 complexes with no significant blue-shifting.²² In the case of naphthalene inclusion (such as in modified cyclodextrins), the observed fluorescence enhancement is a result of the reduced local polarity experienced by the naphthalene fluorophore within the host cavity as compared to in the aqueous solution. In the case of phenyl inclusion, a different mechanism for fluorescence enhancement is required, which involves reduction of the intramolecular rotation freedom of the phenyl ring relative to the naphthalene ring caused by the phenyl inclusion into the large Q7 host.^{44,45} This results in a decrease in the rate of intramolecular charge transfer, which requires an intramolecular twisting of the phenyl ring relative to the naphthalene fluorophore. This charge transfer, followed by energy transfer, represents a significant nonradiative decay pathway for anilinonaphthalenes in polar environments.²² The reduction of the rate for this process reduces the overall rate for nonradiative decay of the 2,6-ANS excited state, resulting in an increase in the fluorescence quantum yield, and therefore the measured fluorescence enhancement.

These fluorescence results for 2,6-ANS in Q7 can be compared to the reported results for 2,6-ANS in Q6,²² allowing for a direct comparison of the host properties of these two cucurbiturils with the same guest. The maximum fluorescence enhancement of 25 observed here for Q7 is significantly larger than the value of 5 reported for Q6, indicating that inclusion of the phenyl group into the larger Q7 results in a much greater reduction in the rate of the charge transfer decay process. Furthermore, the association constant for 2,6-ANS with Q7 of $600 \pm 150 \text{ M}^{-1}$ is more than an order of magnitude larger than that of $52 \pm 10 \text{ M}^{-1}$ reported for 2,6-ANS in Q6. This indicates that a much stronger complex is formed between 2,6-ANS and Q7 as compared to Q6, with ΔG° of inclusion values of -9.7 and $-15.8 \text{ kJ mol}^{-1}$ for Q6 and Q7, respectively. Thus, the larger cavity and portal of Q7 make it a much better host for 2,6-ANS than Q6, giving a much larger fluorescence enhancement as well as a much stronger inclusion complex.

The interaction of 1,8-ANS in Q7 is very different than that of 2,6-ANS. The fluorescent enhancement of 110 is much larger than the 25 observed for 2,6-ANS, as is the observed blue-shift of 48 nm for 1,8-ANS compared to 7 nm for 2,6-ANS. Furthermore, the enhancement versus Q7 concentration data and double reciprocal plot clearly indicate the formation of higher-order inclusion complexes than the simple 1:1 complexes indicated for 2,6-ANS. The data fit extremely well to eq 2 for stepwise 2:1 inclusion, but did not fit well to equations based on either simple 1:1 inclusion or 2:2 inclusion scenarios. Thus the formation of a 2:1 Q7:1,8-ANS complex is strongly indicated, initially believed to be via inclusion of both the phenyl and naphthyl moieties into separate Q7 hosts. However, the NMR results do not support such an inclusion scenario: no shifting of the ^1H NMR signals for the naphthyl protons was

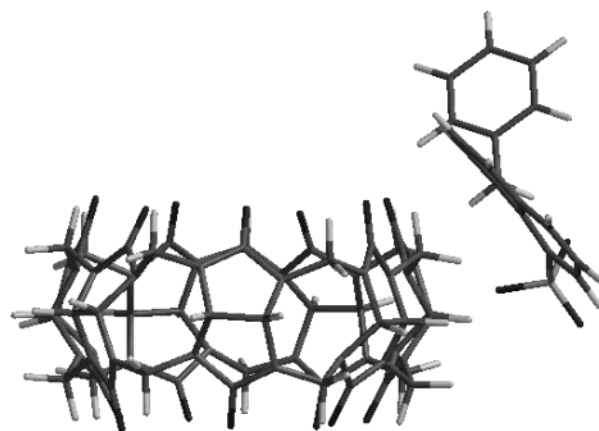


Figure 7. PM3 minimized structure of 1,8-ANS-Q7, starting with the naphthalene moiety inside the cavity.

observed in the 1,8-ANS spectrum as Q7 was added. In fact, the shifting of the phenyl signals clearly observed in the case of 2,6-ANS with added Q7 was also not observed, indicating that neither the naphthyl nor the phenyl moieties are included in the Q7 cavities in the case of 1,8-ANS.

We thus propose the formation of a 2:1 *exclusion* complex in the case of Q7 with 1,8-ANS, involving an external association of 1,8-ANS to the outside of the Q7 hosts. This type of complexation could still explain the large fluorescence enhancement observed, if it were primarily the naphthalene moiety of the 1,8-ANS complexing between the outer surfaces of the two Q7 macrocycles, one on each side. A sandwich complex of this type would dramatically reduce the polarity of the local environment experienced by the naphthalene fluorophore and significantly shield it from water molecules. Such a complex would be stabilized by van der Waals intermolecular forces, as well as interaction of the Q7 exterior with the π -electrons of the naphthalene ring.

This proposed exclusion complex is reminiscent of the lattice inclusion compound we previously reported that forms spontaneously upon mixing of 1,8-ANS and Q6 in solution.³⁹ The main difference in the case of Q7 would appear to be the solubility of the complex: unlike the case of Q6, the complex is soluble at the low 1,8-ANS concentration of $2 \times 10^{-5} \text{ M}$ used in the fluorescence studies, but does precipitate at the higher 1,8-ANS concentrations required in the NMR studies. This may be a result of increased solubility of the Q7 complex as compared to the Q6 complex. Furthermore, the strongly blue-shifted spectrum of 1,8-ANS in the presence of Q7, with a maximum at 469 nm, is similar to that reported for the Q6 exclusion solid, which has a maximum of 478 nm. This supports the idea that external complexation of the 1,8-ANS naphthalene moiety to Q7 would result in strong fluorescence enhancement and blue-shifting.

The proposed lack of inclusion of 1,8-ANS in Q7 was further supported by molecular modeling calculations (PC SpartanPro PM3), in which the 1,8-ANS guest is always pushed to the outside of the Q7, regardless of whether the complex is started with the phenyl or naphthalene moiety inside the cavity, and shows external association as illustrated in Figure 7. These minimized structures are similar to the structure of the 1,8-ANS: Q6 lattice inclusion solid as determined by X-ray crystallography.³⁹

These major differences in complexation of 1,8- and 2,6-ANS with Q7 can be explained by a consideration of the differing geometry of the two ANS isomers, as shown in Figure 1. Both isomers contain a central naphthalene fluorophore; the

differences lie in the position of the anilino and sulfonate substituents on this naphthalene. In general, naphthalene and its derivatives can be included into host cavities in two distinct ways: *axial* inclusion, in which the naphthalene ring enters the cavity via its short dimension, and *equatorial* inclusion, in which the naphthalene ring enters the cavity via its long dimension. 2,6-ANS is long and streamlined, with the anilino and sulfonate groups on opposite ends of the long axis of the central naphthalene. Thus, the sulfonate group does not affect complexation of the phenyl group. However, these two groups effectively prevent both axial and equatorial inclusion of the naphthalene ring. In the case of 1,8-ANS, the presence of both groups on one long side of the central naphthalene allows for unimpeded equatorial inclusion of the naphthalene, although axial inclusion is still impeded. However, such equatorial inclusion of naphthalene into the Q7 cavity is not observed, presumably due to the size mismatch between the Q7 portal and the naphthalene long axis. Furthermore, as mentioned above, the presence of the sulfonate group next to the anilino group may affect inclusion of the phenyl group, via its steric bulk and/or charge distribution. Thus, the geometric differences in these two isomers result in the completely different complexation by Q7 described above: 1:1 inclusion in the case of 2,6-ANS; 2:1 exclusion in the case of 1,8-ANS. We observed nearly identical results for these two probes with Q6.^{22,39} In the case of 2,6-ANS, a 1:1 host-guest complex was observed in solution,²² whereas in the case of 1,8-ANS, a solid lattice inclusion compound was formed. These differences were also explained by the differing geometry of the two probes. Apparently the increased size of the cavity and portal in the case of Q7 as compared to Q6 is still not enough to allow for naphthalene equatorial inclusion; this was also suggested by the molecular modeling studies, in which naphthalene initially included equatorially was quickly found to reorient axially.

Conclusion

Q7 strongly enhances the fluorescence of both 2,6- and 1,8-ANS. In the case of 2,6-ANS, 1:1 inclusion complexes are formed via inclusion of the phenyl moiety into the Q7 cavity (as confirmed by NMR), with a large fluorescence enhancement of a factor of 25 ± 3 and an association constant of $600 \pm 150 \text{ M}^{-1}$. These values are significantly larger than those reported in the literature for 2,6-ANS inclusion into Q6; for example the association constant is larger by over an order of magnitude. This is significant, as it provides the first direct comparison of the host abilities of these two cucurbit[*n*]urils. For this guest, the larger host cavity of Q7 as compared to Q6 results in greatly improved host abilities, both in the strength of the complex formed and in the degree to which the guest fluorescence is enhanced. In the case of 1,8-ANS, very large fluorescence enhancement is also observed upon addition of Q7. The enhancement as a function of Q7 concentration indicates the formation of 2:1 host:guest complexes. However, host-guest inclusion is not observed via NMR, and molecular modeling also indicates that inclusion of 1,8-ANS via either the phenyl or naphthalene moiety does not give a stable complex. Thus, a 2:1 complex where 1,8-ANS is sandwiched between the outer surface of two Q7 molecules is proposed. The naphthalene fluorophore of the 1,8-ANS in such a complex would be significantly shielded from water molecules and experience a significantly less polar microenvironment as compared to free 1,8-ANS in aqueous solution, resulting in the observed significant fluorescence enhancement upon complexation.

Experimental Section

Materials. The following compounds were obtained from the indicated sources and used as received: 1-anilinonaphthalene-8-sulfonic acid (Molecular Probes), 2-anilinonaphthalene-6-sulfonic acid (Molecular Probes); potassium monobasic phosphate (Fisher), potassium dibasic phosphate (Fisher), and sodium sulfate (Fisher). Q7 was prepared according to the procedures described by Day et al.⁴⁶ Drying of samples of Q7 in a vacuum oven showed a water content of 16%; this value was used to correct the concentration of all Q7 solutions.

Fluorescence Spectroscopy. All absorption and fluorescence measurements were performed on solutions in 1 cm² quartz cuvettes. Absorption spectra were measured on a Cary 50 Bio UV-visible spectrophotometer. Fluorescence spectra were measured on a Photon Technologies International LS-100 luminescence spectrometer, with excitation and emission monochromator band-passes set at 3 nm and an excitation wavelength of 370 nm. Solutions were made in a 0.062 M KH₂PO₄/0.038 M K₂HPO₄ buffer (measured pH = 6.80) prepared from ultrapure distilled, deionized water. Solution concentrations were adjusted to give an absorbance of 0.30 at the excitation wavelength: $2 \times 10^{-5} \text{ M}$ (1,8-ANS) and $9 \times 10^{-5} \text{ M}$ (2,6-ANS). Weak fluorescence was observed from Q7 solutions in the absence of ANS; to correct for this, the total fluorescence of a solution containing only Q7 (at the appropriate concentration) was subtracted from the total fluorescence of each solution containing 2,6- or 1,8-ANS and Q7.

NMR Spectroscopy. All NMR spectra were performed on a Varian Unity 400 in D₂O with KD₂PO₄/K₂DPO₄ buffer (pH = 6.80, 0.025 M) and externally referenced. In the 2,6-ANS ($4.6 \times 10^{-3} \text{ M}$ 2,6-ANS) binding studies precipitation was observed to occur at approximately 1:1 Q7/2,6-ANS. Due to solubility problems, saturated solutions of 1,8-ANS were used and even for 2:1 Q7/1,8-ANS no perturbations of the 1,8-ANS spectra were observed.

Molecular Modeling. Molecular modeling studies were performed using semiempirical methods and the PM3 basis set in PC-Spartan Pro software. When the potential binding of 1,8-ANS by Q7 was investigated, no cavity binding of the 1,8-ANS was found despite the use of multiple starting geometries. For 2,6-ANS we calculated the binding energy to be $\sim 35 \text{ kJ mol}^{-1}$ with the phenyl ring encapsulated in the Q7 cavity. It should be noted that all calculations were performed on the zwitterionic forms of 1,8-ANS and 2,6-ANS and calculated as isolated entities in the gas phase.

Acknowledgment. Financial support for this work was provided by the Natural Sciences and Engineering Research Council of Canada (NSERC) and by the UPEI Senate Committee on Research.

References and Notes

- (1) Freeman, W. A.; Mock, W. L.; Shih, N.-Y. *J. Am. Chem. Soc.* **1981**, *103*, 7367–7368.
- (2) Cintas, P. *J. Incl. Phenom. Mol. Rec. Chem.* **1994**, *17*, 205–220.
- (3) Mock, W. L. *Top. Curr. Chem.* **1995**, *175*, 1–24.
- (4) Mock, W. L. *Comprehensive Supramolecular Chemistry* Vol. 2; Vogtle, F., Ed.; Elsevier Science: Oxford, 1996; pp 477–493.
- (5) Mock, W. L.; Shih, N.-Y. *J. Org. Chem.* **1983**, *48*, 3618–3619.
- (6) Mock, W. L.; Shih, N.-Y. *J. Org. Chem.* **1986**, *51*, 4440–4446.
- (7) Mock, W. L.; Shih, N.-Y. *J. Am. Chem. Soc.* **1989**, *111*, 2697–2699.
- (8) Mock, W. L.; Pierpont, J. *J. Chem. Soc., Chem. Commun.* **1990**, 1509–1511.
- (9) Jeon, Y.-M.; Kim, J.; Whang, D.; Kim, K. *J. Am. Chem. Soc.* **1996**, *118*, 9790–9791.
- (10) El Haouaj, M.; Ko, Y. H.; Luhmer, M.; Kim, K.; Bartik, K. *J. Chem. Soc., Perkin Trans. 2* **2001**, 2104–2108.

- (11) El Haouaj, M.; Luhmer, M.; Ko, Y. H.; Kim, K. Bartik, K. *J. Chem. Soc., Perkin Trans. 2* **2001**, 804–807.
- (12) Marquez, C.; Nau, W. M. *Angew. Chem., Int. Ed.* **2001**, *40*, 3155–3160.
- (13) Freeman, W. A. *Acta Crystallogr.* **1984**, *B40*, 382–387.
- (14) Whang, D.; Heo, J.; Park, J. H.; Kim, K. *Angew. Chem., Int. Ed.* **1998**, *37*, 78–80.
- (15) Meschke, C.; Buschmann, H.-J.; Schollmeyer, E. *Thermochim. Acta* **1997**, *297*, 43–48.
- (16) Buschmann, H.-J.; Jansen, K.; Meschke, C.; Schollmeyer, E. *J. Sol. Chem.* **1998**, *27*, 135–140.
- (17) Buschmann, H.-J.; Jansen, K.; Schollmeyer, E. *Thermochim. Acta* **1998**, *317*, 95–98.
- (18) Buschmann, H.-J.; Jansen, K.; Schollmeyer, E. *J. Incl. Phenom. Macro. Chem.* **2000**, *37*, 231–236.
- (19) Hoffmann, R.; Knoche, W.; Fenn, C.; Buschmann, H.-J.; *J. Chem. Soc., Faraday Trans.* **1994**, *90*, 1507–1511.
- (20) Buschmann, H.-J.; Schollmeyer, E. *J. Incl. Phenom. Mol. Recog. Chem.* **1997**, *29*, 167–174.
- (21) Neugebauer, R.; Knoche, W. *J. Chem. Soc., Perkins Trans. 2* **1998**, 529–534.
- (22) Wagner, B. D.; Fitzpatrick, S. J.; Gill, M. A.; MacRae, A. I.; Stojanovic, N. *Can. J. Chem.* **2001**, *79*, 1101–1104 2001.
- (23) Kim, J.; Jung, I.-S.; Kim, S.-Y.; Lee, E.; Kang, J.-K.; Sakamoto, S.; Yamaguchi, K.; Kim, K. *J. Am. Chem. Soc.* **2000**, *122*, 540–541.
- (24) Day, A. I.; Blanch, R. J.; Arnold, A. P.; Lorenzo, S.; Lewis, G. R.; Dance, I. *Angew. Chem., Int. Ed.* **2002**, *41*, 275–277.
- (25) Flinn, A.; Hough, G. C.; Stoddart, J. F.; Williams, D. J. *Angew. Chem., Int. Ed. Engl.* **1992**, *31*, 1475–1477.
- (26) Buschmann, H.-J.; Cleve, E.; Jansen, K.; Schollmeyer, E. *Anal. Chim. Acta* **2001**, *437*, 157–163.
- (27) Buschmann, H.-J.; Cleve, E.; Jansen, K.; Wego, A.; Schollmeyer, E. *J. Incl. Phenom. Macro. Chem.* **2001**, *40*, 117–120.
- (28) Jansen, K.; Buschmann, H.-J.; Wego, A.; Döpp, D.; Mayer, C.; Drexler, H.-J.; Holdt, H.-J.; Schollmeyer, E. *J. Incl. Phenom. Macro. Chem.* **2001**, *39*, 357–363.
- (29) Buschmann, H.-J.; Cleve, E.; Jansen, K.; Wego, A.; Schollmeyer, E. *Mater. Sci. Eng. C* **2001**, *14*, 35–39.
- (30) Kim, H.-J.; Heo, J.; Jeon, W. S.; Lee, E.; Kim, J.; Sakamoto, S.; Yamaguchi, K.; Kim, K. *Angew. Chem., Int. Ed.* **2001**, *40*, 1526–1528.
- (31) Kim, S.-Y.; Jung, I. S.; Lee, E.; Kim, J.; Sakamoto, S.; Yamaguchi, K.; Kim, K. *Angew. Chem., Int. Ed.* **2001**, *40*, 2119–2121.
- (32) Jon, S. Y.; Ko, Y. H.; Park, S. H.; Kim, H.-J.; Kim, K. *Chem. Commun.* **2001**, 1938–1939.
- (33) Lorenzo, S.; Day, A.; Craig, D.; Blanch, R.; Arnold, A.; Dance, I. *Cryst. Eng. Comm.* **2001**, *49*, 1–7.
- (34) Marquez, C.; Nau, W. M. *Angew. Chem., Int. Ed.* **2001**, *40*, 4387–4390.
- (35) Blanch, R. J.; Sleeman, A. J.; White, T. J.; Arnold, A. P.; Day, A. I. *Nano Lett.* **2002**, *2*, 147–149.
- (36) Kim, H.-J.; Jeon, W. S.; Ko, Y. H.; Kim, K. *Proc. Nat. Acad. Sci.* **2002**, *99*, 5007–5011.
- (37) Ong, W.; Gómez-Kaifer, M.; Kaifer, A. E. *Org. Lett.* **2002**, *4*, 1791–1794.
- (38) Zhang, K.-C.; Mu, T.-W.; Liu, L.; Guo, Q.-X. *Chin. J. Chem.* **2001**, *19*, 558–561.
- (39) Wagner, B. D.; MacRae, A. I. *J. Phys. Chem. B* **1999**, *103*, 10114–10119.
- (40) Muñoz de la Peña, A.; Salinas, F.; Gómez, M. J.; Acedo, M. I.; Sánchez Peña, M. *J. Incl. Phenom. Mol. Rec. Chem.* **1993**, *15*, 131–143.
- (41) Nigam, S.; Durocher, G. *J. Phys. Chem.* **1996**, *100*, 7135–7142.
- (42) Hamai, S.; Hatamiya, A. *Bull. Chem. Soc. Jpn.* **1996**, *69*, 2469–2476.
- (43) Wagner, B. D.; Fitzpatrick, S. J. *J. Incl. Phenom. Macro. Chem.* **2000**, *38*, 467–478.
- (44) Kosower, E. M.; Dodiuk, H.; Tanizawa, K.; Ottolenghi, M.; Orbach, N. *J. Am. Chem. Soc.* **1975**, *97*, 2167–2178.
- (45) Kosower, E. M.; Dodiuk, H.; Kanety, H. *J. Am. Chem. Soc.* **1978**, *100*, 4179–4188.
- (46) Day, A.; Arnold, A. P.; Blanch, R. J.; Snushall, B. *J. Org. Chem.* **2001**, *66*, 8094–8100.